

Research on Inverse Kinematics and Block Grasping Techniques for Six-Axis Robotic Arms

Zirui Ren¹, Lisheng Zhang^{2,a,*}

¹Guanghua Cambridge International School, Pudong New Area, Shanghai, China.

²Ulink College of Shanghai, Songjiang District, Shanghai, China

a. Lisheng.Zhang@ulink.cn

*corresponding author

Abstract: Nowadays, large to a variety of factories and aerospace fields, small to mechanical toys, robotic arm has widely used in all works of life. Because of the interest of robotic arms, during the summer vacation, we did some research on the robot arm in order to better understand the operating principle of the robot arm and how to execute the task. This paper discusses the body frame and kinetic principles of a six-degree swivel manipulator arm. We confine to the High-Level APIs that ROS provides and focus this article on the analysis of mechanical design in a robotic arm using inverse kinematics theories. These theories not only help us recognize what goes on in the movement patterns of a robot arm but also for its well-considered control. There are unavoidable slight deviations in the calculation of inverse kinematics and the catching of objects. Even though, through some theories and program, we have already manipulate the robotics to finished some tasks.

Keywords: inverse kinematics, block grasping, six-axis manipulator.

1. Introduction

In this era of rapid technological advancement, robotic arms have emerged as a paragon of automation technology, becoming an indispensable part of industrial production, scientific research, and even everyday life [1,2]. They are not merely machines; they are the epitome of precision engineering, intelligent control, and innovative design. Robotic arms, as automated robotic devices capable of performing pre-programmed tasks, explore the linear relationship between the virtual values of the manipulator and the specific values of the degrees of freedom through precise mathematical models and advanced algorithms, providing a solid theoretical foundation for complex tasks such as object grasping. The construction of a robotic arm typically consists of multiple joints connected by mechanical structures, enabling flexible movement and object manipulation in three-dimensional space. This is the result of the integration of knowledge and technology from various disciplines, including mechanical engineering, control engineering, and electronic engineering. With the continuous advancement of sensor technology, computational capabilities, and control algorithms, the performance of modern robotic arms has been increasingly enhanced, and the tasks they can handle have become more complex and sophisticated [3].

Particularly noteworthy is the advent of First-Person View (FPV) robotic arms, which ingeniously combine drone technology with robotic arm operation, providing operators with a new intuitive way of operation. Through FPV technology, robotic arms can recognize colors, determine the location of

objects, and even perform tasks in complex environments, undoubtedly opening up new possibilities for the application of robotic arms [4]. The core objective of this project is to construct and practice a six-degree-of-freedom robotic arm, which not only involves an in-depth understanding of mechanical structures and joint design, such as gear mechanisms and screw-nut connections, but also covers basic motion modes, operation methods, and the impact of each degree of freedom on the overall movement. By utilizing APP software and "NoMachine" for remote control, the project further explores forward and inverse kinematics, using trigonometric functions and matrix algebra to efficiently position the robot's end-effector.

In addition, the project includes the construction and debugging of control systems, the integration of hardware and software for precise control, and the analysis of experimental data to evaluate the performance of the robotic arm and identify issues to be resolved.

In the subsequent sections, we will delve into the critical knowledge of robotic arm design and implementation in three parts. Sections 3.1 to 3.3 will elaborate on the hardware configuration in detail. Chapter 4 will delve into the process implementation, which involves translating the design into a functioning robotic arm system, with a primary focus on the analysis of forward and inverse kinematics principles.

2. Design and implementation

2.1. System architecture

The robotic arm, a critical component of the entire system, is designed to perform specific actions and tasks. Typically, it consists of multiple parts, such as motor-driven rotary joints, and possesses a designated number of degrees of freedom, enabling versatile movement. The control system, which governs the robotic arm, is managed by electronic and computational devices. This system comprises a main controller, responsible for motion planning and execution; a sensor interface, which gathers real-time data from various sensors like position and force sensors; and drivers, which convert the commands from the main controller into mechanical motions through components such as motors and actuators [1].

An essential feature of the robotic arm is its FPV module camera, which provides real-time live video of the arm's operation. This video transmission allows offsite operators and automation systems to monitor and control the robotic arm [2]. To facilitate remote control and monitoring, the communication module includes a wireless communication unit, supporting WiFi or Bluetooth connectivity.

In terms of hardware design, the construction of the robotic arm involves several key servos, each with specific functions and material requirements. The base servo controls the first joint, known as the rotary joint, allowing horizontal rotation. For this, materials with high load-bearing stability, such as aluminum alloy, steel, or other high-strength metals, are used. The shoulder servo, which manages the second joint, requires high-strength metals or alloys to maintain structural integrity while balancing weight and stability. The elbow servo, responsible for the third joint, enables the arm to bend in a plane, using materials similar to those of the base servo to ensure stability during bending. The wrist rotation servo, controlling the fourth joint, allows for horizontal rotation at the wrist and employs materials as strong and stable as those used in the base servo (Figure 1). The wrist tilt servo, which tips the end of the robotic arm at the fifth joint, uses high-strength alloys or special engineering plastics to meet the mechanical requirements. Lastly, the end effector servo, which controls the final part of the arm, including fixtures and sensors, is selected based on specific application needs, potentially incorporating special alloys, plastics, and electronic components (Figure 2) [3].

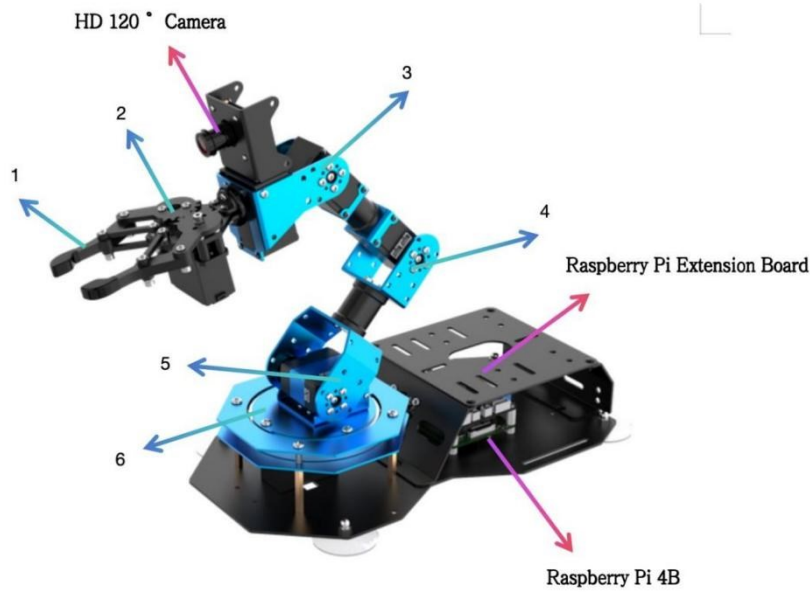


Figure 1: The construction of robotic arm [3]

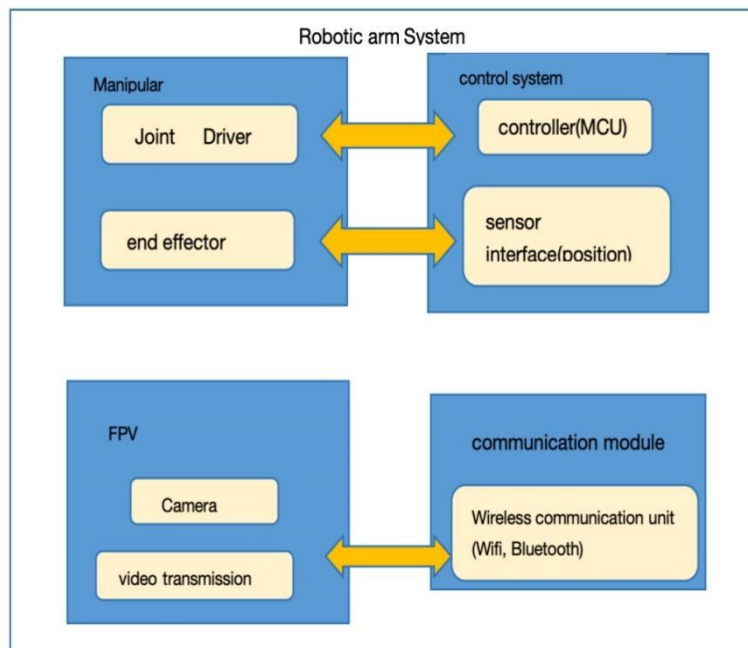


Figure 2: The structure of robotic arm system [3]

2.2. Dof configuration

The robotic arm's design incorporates six critical degrees of freedom for enhanced maneuverability and precision: base rotation for 360-degree horizontal movement, shoulder elevation for height adjustment with a high-torque servo motor, elbow rotation for vertical plane changes, wrist elevation for vertical end-effector positioning with a linear actuator, wrist rotation for horizontal direction changes, and gripper opening/closing for object manipulation. Each joint is equipped with high-precision components such as servo motors with torque ranging from 3 to 8 Nm and resolution of

0.01 degrees, along with linear guides and position feedback sensors, to ensure reliable operation and accurate control in diverse applications (Table 1) [4].

Table 1: Dof configuration detail

Degree of Freedom	Function Description	Range of Motion	Configuration Recommendations	Example Configuration
Base Rotation	Rotates the end-effector on a horizontal plane for 3D object manipulation.	360 degrees	High-precision servo motor; secure mounting; high-quality bearings for reduced friction.	Servo Motor: 5 Nm torque, 0.01-degree resolution; quality bearings.
Shoulder Elevation	Adjusts height; defines reach range of the robotic arm.	Lowest to highest point	High-torque, low-backlash servo motor with gear reduction to enhance torque and control.	Servo Motor: 8 Nm torque, 0.01-degree resolution; gear ratio 20:1.
Elbow Rotation	Facilitates angle changes by rotating around a vertical plane.	Specified angular range	Accurate angle sensors and servo motors for rotational control; sufficient torque.	Servo Motor: 4 Nm torque, 0.01-degree resolution; ± 0.1 -degree angle sensor accuracy.
Wrist Elevation	Moves the end-effector up and down in a vertical plane.	Lowest to highest point	Servo motor with good linear characteristics; linear guide to improve stability and accuracy.	Linear Actuator: 200 N thrust; integrated linear guide.
Wrist Rotation	Rotates the end-effector on a horizontal plane.	360 degrees	Suitable servo motors and bearings for smooth, accurate rotation.	Servo Motor: 3 Nm torque, 0.01-degree resolution; precision bearings.
Gripper Opening/Closing	Opens and closes to pick up or drop objects.	Fully closed to fully open	Choose gripper type (parallel, needle) and actuation mechanism (pneumatic, electric, hydraulic) based on the application.	Electric Gripper: 100 N clamping force; includes position feedback sensor.

In the FPV module, the key components include: a high-resolution, low-latency, and wide-angle camera (e.g., 1080p resolution, 60 fps frame rate, and a 120-degree wide-angle lens) for capturing and transmitting real-time images; a video transmitter operating at 5.8 GHz (e.g., 25 mW power and supporting 8 channels) to ensure long-range and low-latency stable image transmission; a receiver with high sensitivity and strong anti-interference capabilities (e.g., a 5.8 GHz receiver with automatic channel search functionality) to convert radio signals into image signals; a lightweight, high-resolution, and low-latency display device (e.g., a 7-inch, 1280x720 resolution, portable display with latency less than 50 ms) for presenting the images to the user; and a controller with an intuitive interface and strong compatibility (e.g., a multifunctional controller with a touchscreen interface and customizable settings) to allow the user to control camera angles, frequency switching, and other

functions. These components work together to provide a reliable and immersive real-time monitoring and control experience (Table 2).

Table 2: FPV module

Component	Function Description	Configuration Recommendations	Example Configuration
Camera	Captures real-time images and transmits them to video devices.	Choose a camera with high resolution, low latency, and a wide field of view for optimal performance.	1080p resolution, 60 fps, 120-degree wide-angle lens.
Video Transmitter	Sends the captured images from the camera to a display device.	Select a transmitter operating at 5.8 GHz with long-range and low-latency capabilities to ensure stable transmission.	25 mW, supports 8 channels.
Receiver	Converts the radio signals from the transmitter into image signals for display.	Choose a receiver with high sensitivity and strong anti-interference capabilities to ensure smooth transmission.	5.8 GHz receiver with automatic channel search functionality.
Display Device	Displays the received images to the user.	Select a lightweight, high-resolution, and low-latency display to provide an immersive experience.	7-inch, 1280x720 resolution, portable display with latency < 50 ms.
Controller	Allows users to control camera angles, frequency switching, and other functions.	Choose a controller with an intuitive interface and strong compatibility to enhance usability.	Multifunctional controller with a touchscreen interface and customizable settings.

3. Implementation process

3.1. Introduction of forward kinematic and inverse kinematic

In robotic arm systems, kinematics is used to describe the motion of the arm's joints and their relationship to the end-effector's position in space. Forward kinematics involves determining the position of the end-effector when all joint angles are known, while inverse kinematics entails calculating the necessary joint angles to place the end-effector in a desired position. Both are essential for robotic control and are widely used to ensure precision and accuracy in movement.

- **Introduction to Forward Kinematics**

In robot kinematics, forward kinematics refers to the use of the kinematic equations of a robot to compute the position of the end-effector from specified values of the joint parameters [5]. This process allows for the determination of the end-effector's position and orientation based on the given joint angles.

- **Introduction to Inverse Kinematics**

In computer animation and robotics, inverse kinematics (Figure 3) is the mathematical process of calculating the variable joint parameters required to place the end of a kinematic chain, such as a

effector: $CP = z + L4 \sin(\alpha) - L1$ This gives the vertical distance based on the height z , adjusted for the arm's length $L4$ and initial height $L1$. AC : Using the Pythagorean theorem, we calculate the distance between the base and the end-effector in 3D space

3.3. Angle calculation using inverse kinematics

The different angle tells the joint of robotic arm how far and in which direction one segment will move. The angle solutions have to be used to control the arm in such a way that it moves smoothly, quickly, but still within the boundaries of its physical ability. The angles θ_4 , θ_5 and θ_6 can be derived using the angles of AC , AP and CP values.

Using the values of AC , AP , and CP , the angles θ_4 , θ_5 , and θ_6 can be calculated. For example, using the cosine rule, the angle θ_4 can be computed as: $\theta_4 = 180^\circ - \cos^{-1} \left(\frac{L_2^2 + L_3^2 - AC^2}{2L_2L_3} \right)$ This calculation represents the relationship between the various arm segments L_2 , L_3 , and the distance AC , allowing precise control of the elbow joint. Similarly, we can calculate angles like θ_5 and θ_6 using trigonometric functions such as: This angle controls the arm's vertical positioning. Finally, the angle θ_6 can be derived by considering the orientation of the arm's end-effector relative to the base: $\theta_6 = \cos^{-1} \left(\frac{L_2^2 + L_3^2 - AC^2}{2L_2L_3} \right)$.

3.4. Practical application of kinematics

Every one of these angles is crucial for calculating the precise movement and positioning of the robotic arm. As the inverse kinematics approach is not limited to single joints, it can integrate geometric and physical constraints of the whole system. The robotic arm moves very smoothly and precisely if all these calculations are combined, thus it is capable of perfect motion for tasks like object manipulation or precise placement.

The equations and principles described above ensure that each joint operates within its range while maintaining the necessary stability and accuracy. To date, the robotic arm can move to a specific position given the coordinates (x, y, z) . As the project aims to grasp blocks from three different locations ($place_1$, $place_2$, and $place_3$) and place them in corresponding areas based on their color, the camera of the robotic arm must be able to detect the color of the blocks. For this purpose, a library named "CV2" (OpenCV) needs to be imported. Each time the robotic arm grasps a block, it will appear at the bottom of the camera's field of view. A function is defined to detect the RGB color of the area at the bottom of the camera. This function is called every time the block is grasped, and it returns the detected RGB value [8].

After obtaining the RGB value, the robotic arm compares the detected RGB with the predefined ranges for red, blue, and green to determine the color of the block. Once the color is determined, the robotic arm can place the block in the corresponding designated area [9].

4. Result and discussion

The experiments are tested on a robotic arm system that runs the Raspberry Pi platform. We performed a series of tests to determine if the camera could properly identify object colors and verify that our model was capable of producing accurate and consistent results. The experimental data obtained under this system method had made the foundation of various conclusions from the ensuing tests.

4.1. Colour recognition test

The experiment aimed to ascertain the camera's capability to detect and identify color signals from wooden blocks painted in red, green, and blue colors by analyzing their RGB values within predefined optical boundaries. The protocol involved placing each wooden block individually within the camera's field of view to record their RGB values, which were then compared against the anticipated values for accuracy. The results indicated that the camera successfully identified the RGB values for each color block, aligning with the data presented in the table 3. This demonstrated that the color of each block was accurately recognized, affirming that the system is equipped with a precise color recognition algorithm.

Table 3: experimental data for color recognition

image	RGB	result	Truth value
image. Red	(219,21,79)	red	Red
image. Green	(0,115,51)	green	Green
image. Blue	(-20,131,164)	blue	Blue

4.2. Block grasping test

The objective of the experiment was to verify whether a robotic arm could calculate the necessary pulse values for each of its servos to properly grip a block, based on 3D coordinates provided. The procedure involved using 3D coordinates to locate and instruct the robotic arm to move to the position of each block, grasp it, and then move it to a different location. The results showed that in all six sets of data, the robotic arm was successful in grabbing the blocks after accurately determining the pulse values from the 3D coordinates (Table 4). The positioning accuracy was within an error margin of less than 0.2 cm, although minor deviations were observed, which could be attributed to slight hardware looseness. These findings confirm the effectiveness of the previously described inverse kinematic model.

Table 4: Experimental data for forward kinematic

theta3	theta4	theta5	theta6	alpha	cartesian coordinate	real coordinate
76	578	326	183	74	(20,5.7,1)	(19.8,5.5,1)
46	549	315	116	77	(20,0,1)	(19.9,0,1)
76	578	326	183	74	(20,-5.7,1)	(20.1,-5.7,0.8)
76	578	326	183	74	(20,5.7,1)	(-20.1,5.7,1)
46	549	315	116	77	(-20,0,1)	(-20,0,1)
76	578	326	183	74	(-20,-5.7,1)	(-20,5.7,0.9)

4.3. Servo pulse control test

The objective of the test was to evaluate the robotic arm's ability to reach specific pre-defined positions by supplying certain pulse values to its servos. The experiment involved inputting six different pulse width (PW) sets into the system, each corresponding to various target positions. The purpose was to determine whether the robotic arm could consistently and accurately reach all the designated positions.

The results were promising, as the robotic arm successfully reached the anticipated positions with precision using all six sets of pulse values (Table 5). This consistency in performance affirms the

robustness and reliability of the forward kinematics model that was previously discussed, demonstrating its effectiveness in translating mathematical models into accurate physical movements of the robotic arm.

Table 5: Experimental data for inverse kinematic

cartesian coordinate	theta3	theta4	theta5	theta6	alpha	real coordinate
(20,5.7,1)	76	578	326	183	74	(20,5.6,1)
(20,0,1)	46	549	315	116	77	(19.9,0,1)
(20,-5.7,1)	76	578	326	183	74	(20,- 5.7,0.8)
(20,5.7,1)	76	578	326	183	74	(- 20.1,5.7,1)
(-20,0,1)	46	549	315	116	77	(-20,0,1)
(-20,-5.7,1)	76	578	326	183	74	(- 20,5.7,0.9)

4.4. Final experiment and results

An experiment has been defined for the purpose of validating that the algorithm model is applicable in practice, where three wooden blocks of different colours (one red, one green and one blue) are placed one by in another inside detection area of the robot arm. The experiment goal was to validate if the robotic arm identified the RGB values of each block correctly in order to pick them up and assemble them on their predefined positions based on color recognition and target coordinates established.

The results from the captured images during the experiment indicate that the robotic arm successfully recognizes and picks up the blocks based on color as well as deliver them to their appropriate locations with precision. Experimental results show the real-world effectiveness of our algorithm model, and prove a high level of reliability in object recognition and manipulation. The availability of this result provides valuable evidence to support the application of the model for task achieving purpose in industry based color discrimination, which confirms its robustness in dynamically working operational environments (Figure 5 and Figure 6).

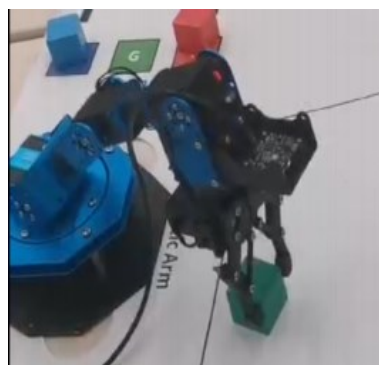


Figure 5: The robot arm identifies the green block (Photo/Picture credit : Original)

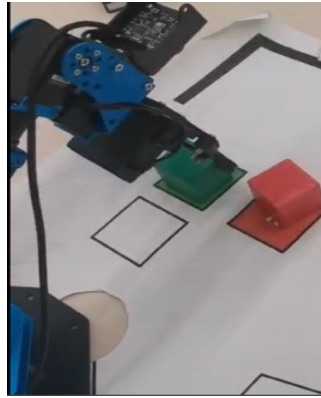


Figure 6: The robot arm places the green block in the predetermined position (Photo/Picture credit : Original)

5. Conclusion

We successfully proposed the algorithmic model of object grasping system with color recognition task utilizing a six water-arm robot in the present paper. Using precise identification and color processing information, the robot can locate objects of any color and grasp them independently ensuring that in actual operations are amplified due to high accurate positioning, flexible application and excellent grasping efficiency. This model has all the sophisticated algorithms for color recognition and object pick/place features to go with it so that the robot can identify same size objects which are of different colors. According to the experimental results, this algorithm model is very robust and can work under very complex & dynamic environments. Its scalability would also help in advancing the design to incorporate into other sophisticated robotic systems. The algorithm model of this can be use at different potential applications. In industrial automation that can be used to sort and handle products of various colors on manufacturing lines, increasing efficiency and savings on labor costs. For instance, in logistics and warehousing, the model might improve on an automated sorting system for various goods. Moreover, in the healthcare field it might help to categorize medical instruments and accessories by color-coded system for increased efficiency on hospital and laboratory operations.

Authors Contribution

All the authors contributed equally and their names were listed in alphabetical order.

References

- [1] Yuan, W., Prasad Poosa, S. R., & Dirks, R. F. (2024). Comparative analysis of color space and channel, detector, and descriptor for feature-based image registration. *Journal of Imaging*, 10 (5), 105
- [2] Zee, L., R., C., Z X., Yang-sheng, L., Nan, H. (2023). Robotic arm three-dimensional printing and modular construction of a meter-scale lattice façade structure. *Engineering Structures*, 290
- [3] Recupito, G., Pecorelli, F., Catolino, G., Lenarduzzi, V., Taibi, D., Di Nucci, D., & Palomba, F. (2024). Technical debt in AI-enabled systems: On the prevalence, severity, impact, and management strategies for code and architecture. *The Journal of Systems and Software*, 216 , 112151.
- [4] Song, J., Wei, J., Yu, B., Liu, C., Ai, C., Zhang, J. (2023). Configuration design and kinematic performance analysis of a novel 4-DOF parallel ankle rehabilitation mechanism with two virtual motion centers. *Chinese Journal of Mechanical Engineering*, 36 (06), 99–116.
- [5] Klein, O. (2023). On forward and inverse uncertainty quantification for a model for a magneto-mechanical device involving a hysteresis operator. *Applications of Mathematics*, 68 , 795–828.
- [6] Pozo-Palacios, J., Fulbright, N. J., Voth, J. A. F., Van de Ven, J. D. (2023). Comparison of forward and inverse cam generation methods for the design of cam-linkage mechanisms. *Mechanism and Machine Theory*, 190 .

- [7] *S,anliturk, I. H., Kocabas, H. (2024). Precise calculation of inverse kinematics of the center of gravity for bipedal walking robots. Applied Sciences, 14 (9).*
- [8] *Yang, X., Liu, Y., Huang, Y., Han, X., Duan, G., Fu, H., Han, J., Zhang, C., He, S., & Jiang, S. (2024). Coordination-driven in-situ controlled synthesis of cellulose-based fluorescent composite with tunable color for decoration, anti-counterfeiting, and accurate color recognition. International Journal of Biological Macromolecules, 134890 .*
- [9] *Sullivan, J. J., Zekelman, L. R., Zhang, F., Juvekar, P., Torio, E. F., Bunevičius, A., Essayed, W. I., Bastos, D., He, J., Rigolo, L., Golby, A. J., & O' Donnell, L. J. (2023). Directionally encoded color track density imaging in brain tumor patients: A potential application to neuro-oncology surgical planning. NeuroImage: Clinical, 38 , 103412.*